Available online at www.sciencedirect.com
SCIENCE DIRECT
Toxicology and Applied Pharmacology 206 (2005) 102–112
Toxicology and Applied Pharmacology
www.elsevier.com/locate/ytaap

Assessment of cytotoxicity by emerging impedance spectroscopy

Caide Xiao, John H.T. Luong*

Biotechnology Research Institute, National Research Council Canada, Montreal, Quebec, Canada H4P 2R2

Received 17 March 2004; accepted 12 October 2004
Available online 30 March 2005

Abstract

An on-line and continuous technique based on electric cell substrate impedance sensing (ECIS) was developed for measuring the concentration and time response function of fibroblastic V79 cells exposed to toxicants. Mercury chloride ($HgCl_2$), cadmium chloride ($CdCl_2$), benzalkonium chloride (BAK), sodium arsenate (Na_2HAsO_4), and trinitrobenzene (TNB) were used as five test models. The first four chemicals serve as a model for acute toxicants, and TNB represents a model for long-term cytotoxicity effects. Adhesion, spreading, and proliferation of V79 fibroblastic cells cultured on a microarray of small gold electrodes precoated with fibronectin were detected as resistance changes. The response function was derived to reflect the resistance change as a result of cell attachment, spreading, mitosis and cytotoxicity effect. Exposure of V79 cells to toxicants led to alterations in cell behavior, and therefore, chemical cytotoxicity was easily screened by measuring the response function of the attached and spread cells in the presence of inhibitor. The half inhibition concentration, the required concentration to achieve 50% inhibition, was obtained from the response function to provide dynamic information about cytotoxicity during the course of the assay. A simple mathematical model was developed to describe the responses of ECIS that were related to the adhesion, spreading, and proliferation of V79 fibroblastic cells. The novel results of this paper are mainly characterized by the systematic study of several parameters including the cell number, detection limit, sensor sensitivity, and cytotoxicity, and they may motivate further research and study of ECIS sensors.

Keywords: Cytotoxicity; Spectroscopy; Toxicant; Impedance; Cell adhesion

Introduction

The tracking of cell adhesion and motility plays an important role in cell biology to elucidate biological phenomena such as cell division, tumor metastasis, and embryonic cell migration. Cell adhesion to connective tissues is the result of the specific binding of integrins to extracellular matrix (ECM) proteins such as fibronectin, laminin and collagen (Bell et al., 1979). Integrins are non-covalently associated heterodimeric transmembrane receptors composed of an α subunit and a β subunit (Fig. 1). There are eighteen α and eight β subunits, and their noncovalent combinations result in the formation of 24 distinct integrins expressed on the cell plasma membrane of diverse cell types (Hynes, 1992; Van der Flier and Sonnenberg, 2001). Integrins are involved in the regulation of a variety of important biological processes, including embryonic development, wound healing, prevention of apoptosis, and tumor metastasis.

Cell attachment is often studied with a radiation label technique (Pickering et al., 2000) which cannot provide dynamic information. Microscopes have been widely used to study cell attachment with the result described only in qualitative terms. For a continuous record of cell adhesion, cinematographic arrangements are necessary and data obtained are very difficult to quantify and usually require image processing with extensive data manipulation. Electric cell-substrate impedance sensing (ECIS) pioneered by Giaever and Keese (1984) is suitable for continuous, automatic, and real-time cell attachment analysis (Fig. 1).

In brief, this technique utilizes an array of small gold electrodes, deposited on the bottom of tissue culture wells and immersed in a culture medium. Upon inoculation with a specific cell line, inoculated cells have a tendency to drift downward and attach to the electrode surface, which is

* Corresponding author.
E-mail address: john.luong@cnrc-nrc.gc.ca (J.H.T. Luong).

0041-008X/$ - see front matter © 2005 Elsevier Inc. All rights reserved.
doi:10.1016/j.taap.2004.10.025

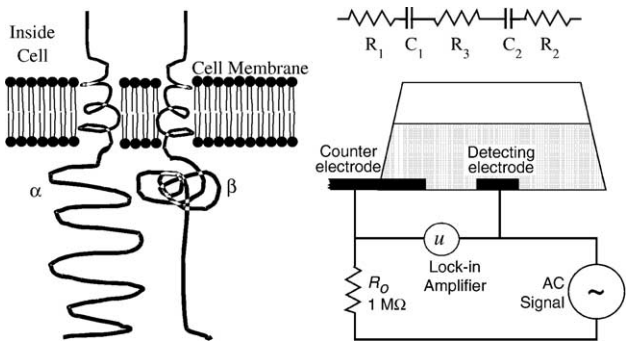

Fig. 1. (Left) Diagram of an integrin, which penetrates through cell membrane. (Right) The circuit of an ECIS and a cell-culture well (~0.9 mL) with a detecting electrode and a counter electrode. An equivalent circuit for the two electrolyte/gold interfaces and the culture medium is also shown in the graph.

normally precoated by a specific protein to promote cell adhesion. The attaching cells will interfere with the free space immediately above the electrode for current flow. When an AC voltage is applied between the two electrodes through a resistance of 1-MΩ, a lock-in amplifier can monitor the voltage between the two electrodes. Owing to its significantly smaller size compared to the counter electrode, the detecting electrode will dominate the overall impedance of the circuit, which can increase as much as 3- to 10-fold in a few hours. The increased impedance, a coordination of many biological reactions within the cell, can be continuously monitored and interpreted to reveal information about cell spreading and micromotion. ECIS has been demonstrated as a useful tool for kinetics and quantitation of mammalian cell spreading and motility as well as an alternative to animal testing for toxicology studies.

The first paper about ECIS was published in 1984, only 1 year later than the first paper about surface plasmon resonance (SPR) biosensors (Liedberg and Nylander, 1983). Hitherto, there are more than 4500 SPR papers compared to 60 ECIS papers. Although ECIS is not widely accepted by biologists, our exploration indicates a potential application of ECIS in cytotoxicity. In this study, we establish a simple mathematical model to describe ECIS responses to the behavior of V79 fibroblastic cells cultured on a microarray of small gold electrodes precoated with fibronectin. A simple and rapid approach is described for on-line monitoring of cell growth and then using cell-substratum interactions as valuable predictors of in vivo response to mercury chloride ($HgCl_2$), cadmium chloride ($CdCl_2$), benzalkonium chloride (BAK), sodium arsenate (Na_2HAsO_4), and trinitrobenzene (TNB) as five test models. The first four chemicals serve as a model for acute toxicants, and TNB represents a model for non-acute but long-term cytotoxicity effects. The inhibition assays provide the inhibitor concentration required to achieve 50% or half inhibition in real time. $HgCl_2$, $CdCl_2$, and Na_2HAsO_4 are the most toxic substances known to humanity. TNB is found at contaminated sites as a by-product during 2,4,6-trinitrotoluene (TNT) production and it can be formed through photochemical oxidative degeneration of TNT manufacturing (U.S. E.P.A., 1997). The Resource Conservation and Recovery Act designates TNB as a hazardous waste when it occurs as a discarded commercial product, off-spec species, or spill residue (Dorsey and Llaods, 1999).

The principle of ECIS

A commercial ECIS system (Applied Biophysics, Troy, NY) is used in this study. It consists of a lock-in amplifier (model SR830, Stanford Research Systems, Sunnyvale, CA), a control box, and a CO_2 incubator. An ECIS sensing chip (model 8W1E, Applied Biophysics, Troy, NY) consists of eight detecting electrodes (0.057 mm^2) deposited on the bottom of eight separate wells. A common counter electrode (7×46 mm^2) is shared by the eight detecting electrodes on the chip with an active area of 2×9 mm^2 in each well. Each detecting electrode and the counter electrode are linked with a pad at the left edge of the chip. These electrodes and pads are thin gold films (50 nm) sputtered on polycarbonate substrates (Keese et al., 1998). A ribbon cable (length of 125 cm) connects a chip in the incubator to the control box under the lock-in amplifier. The ECIS system can process 16 wells on two chips in experiments, but the lock-in amplifier only has one channel. The wells on the two chips are named A_1, $A_2 \ldots A_8$, and B_1, $B_2 \ldots B_8$. By default well A_1 is connected to the lock-in amplifier. After the impedance of well A_1 is measured, the control box automatically connects well A_2, $A_3 \ldots B_8$ to the lock-in amplifier step by step to measure the impedance of all the 16 wells.

Although the impedance of an electrode/gold interface is complex, an equivalent RC circuit could simulate its electric property, but the resistance and capacitance of the equivalent RC circuit might change with frequency. In the equivalent RC circuit of a well filled with culture medium shown in Fig. 1, R_1C_1 and R_2C_2 are the equivalent circuits for the electrode/gold interfaces on the counter electrode and detecting electrode, respectively; R_3 is the resistance of the culture medium between the two interfaces (~800 Ω). The resistance of the well filled with culture medium should be:

$$R_s = R_1 + R_2 + R_3 \tag{1}$$

The capacitance of the well is expressed as

$$C_s = \left(\frac{1}{C_1} + \frac{1}{C_2} \right)^{-1} \tag{2}$$

From the equivalent R_sC_s circuit, the impedance of the well filled with culture medium is:

$$Z_s = R_s - \frac{j}{\omega C_s} \tag{3}$$

Since the capacitance on an electrolyte/gold interface comes from the double electric charge layers on the interface, it is proportional to the area of the electrode. In an ECIS chip, C_1/

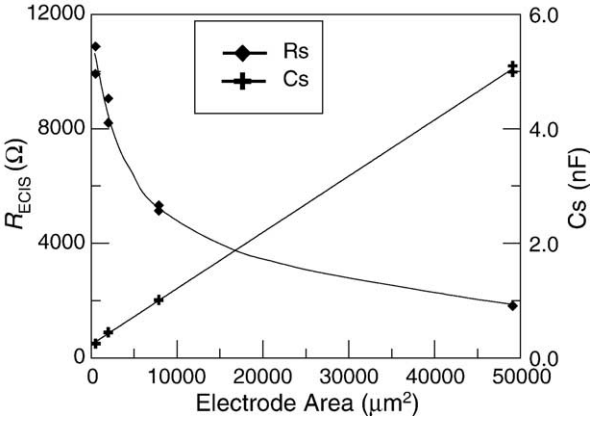

Fig. 2. The equivalent resistance and capacitance of an 8W1E chip with different sizes of detecting electrodes which were in 0.2 mL DMEM plus 5% FBS. The measurements were performed at 4 kHz.

C_2 is about 300 because the area of the counter electrode is about 315 times the area of a detecting electrode. The capacitance on the detecting electrode interface can be used for the capacitance of the well filled with culture medium. As the resistance of the well is inversely proportional to the area of the interface, the resistance of the detecting electrode also dominates the resistance of the well. Fig. 2 showed the resistance and capacitance of an 8W1E chip with different size of detecting electrodes which were in 0.2 mL DMEM and 5% FBS. The measurements were performed at 4 kHz.

In the ECIS circuit shown in Fig. 1, the AC signal amplitude (V_o) is set at 1.0 V, and its frequency (f) could be varied from 25 Hz to 60 kHz. The AC signal in the system is:

$$V = V_o e^{j\omega t} \tag{4}$$

where $j = \sqrt{-1}$ and $\omega = 2\pi f$. Since the AC potential is applied to the detecting and counter electrodes through a 1-MΩ resistor (R_o), the current flowing through the system can be predicted by Ohm's law.

$$I = \frac{V_o}{R_o + Z_s} e^{j\omega t} \tag{5}$$

Also from Ohm's law, the voltage between the two electrodes should be:

$$u_1 = V_o \frac{Z_s}{R_o + Z_s} e^{j\omega t} \tag{6}$$

If $|Z_s| < 0.01\ R_o$, that is, $|Z_s| < 10$ kΩ, the above formula can be simplified as Eq. (7). In this condition, the amplitude of current in the system is in μA scale, and the amplitude of voltage between the two electrodes is in mV scale. This is very important because if current or voltage were too high, cells attached on electrodes would die.

$$u_1 = V_o \frac{Z_s}{R_o} e^{j\omega t} \tag{7}$$

The amplitude (u_o) and phase (φ) of the voltage between the detecting and counter electrodes can be measured directly by the lock-in amplifier:

$$u_2 = u_o e^{j(\omega t + \varphi)} \tag{8}$$

The voltage predicted by Ohm's law (Eq. (7)) and the voltage directly measured by the lock-in phase amplifier (Eq. (8)) should be the same.

$$V_o \frac{Z_s}{R_o} e^{j\omega t} = u_o e^{j(\omega t + \varphi)} \tag{9}$$

Since u_o and φ are known from the lock-in phase amplifier, V_o and R_o are known from the circuit of the ECIS system, the impedance of the well can be directly measured in a condition $|Z_s| < 0.01\ R_o$.

$$Z_s = R_o \frac{u_o}{V_o} e^{j\varphi} = R_o \frac{u_o}{V_o} \cos(\varphi) + jR_o \frac{u_o}{V_o} \sin(\varphi) \tag{10}$$

The equivalent resistance and capacitance of the well can be obtained by comparing Eq. (3) with Eq. (10).

$$R_s = R_o \frac{u_o}{V_o} \cos(\varphi) \tag{11}$$

$$C_s = -\frac{V_o}{\omega R_o u_o \sin(\varphi)} \tag{12}$$

Modification of ECIS

Figs. 3A and B showed the resistance and capacitance directly measured from a commercial ECIS system during cell culture of Chinese hamster lung fibroblast V79 cells (93-CCL) purchased from the American Type Culture Collection (ATCC, Rockville, MD). The measurements were performed at 4 kHz. The lines marked with (1) in the graphs came from a control well filled with 0.2 mL DMEM plus 5% FBS without cells. The resistance of the control well changed very little, but their capacitance increased about 1 nF (about 20% of the background). The lines marked with (2) and (3) in the graphs came from wells filled with cells in the same culture medium. At the end of cell culturing, the resistance and the capacitance of the wells at different frequencies were measured and shown in Figs. 3C and D. For different wells, the higher the resistance of the well was, the lower the capacitance of the well would be. For the same well, both the resistance and capacitance decreased with frequency. Usually, the resistance of a well with cells attached to electrodes would increase with time during cell culture as shown by the lines marked with (3), but sometimes the resistance of the well only increased at beginning of cell inoculation as shown by the line (2) in Fig. 3A.

We used a precise metal film resistor and a ceramic capacitor in series as a sample to see if the measurement of the commercial ECIS system was reliable. We found that the 125-cm cable between a chip and the control box had parasitic impedance (Z_p), which was connected with sample impedance in parallel. An equivalent RC circuit with $R_p = 1$ kΩ and $C_p = 0.2$ nF could be used to simulate

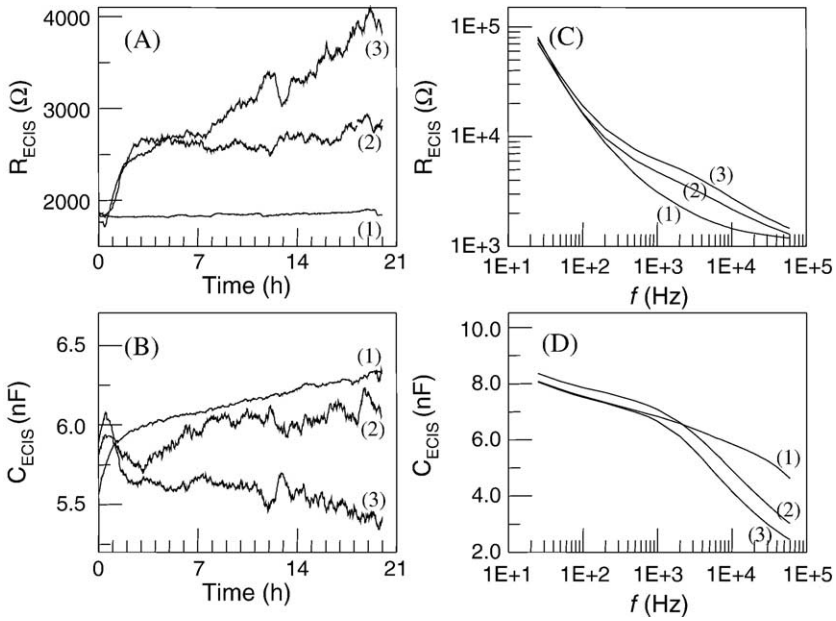

Fig. 3. (A, B) Directly measured impedance of 8W1E wells during cell culture of V79 at 4 kHz; (C, D) directly measured impedance by the end of cell culture at different frequencies. The line (1) came from wells without cell as control, and lines (2) and (3) came from wells with V79 cells attached on electrodes.

the effects of the parasitic impedance to ECIS measurements. For a sample with impedance Z_s measured by the commercial ECIS system, the impedance reported by the machine should be Z_{ECIS}.

$$Z_{ECIS} = \left(\frac{1}{Z_s} + \frac{1}{Z_p}\right)^{-1} \tag{13}$$

$$R_{ECIS} = Re(Z_{ECIS}) = \left(R_s + R_p\right)\frac{\omega^2 R_s R_p C_s C_p - 1 + \frac{C_s + C_p}{R_s + R_p}\left(\frac{R_s}{C_p} + \frac{R_p}{C_s}\right)}{\omega^2\left(R_s + R_p\right)^2 C_s C_p + \frac{\left(C_s + C_p\right)^2}{C_s C_p}} \tag{14}$$

$$C_{ECIS} = \frac{-1}{2\pi f \mathrm{Im}(Z_{ECIS})} = \frac{\omega^2\left(R_s + R_p\right)^2 C_s C_p + \frac{\left(C_s + C_p\right)^2}{C_s C_p}}{\left(1 - \omega^2 R_s R_p C_s C_p\right)\left(\frac{1}{C_s} + \frac{1}{C_p}\right) + \omega^2\left(R_s + R_p\right) C_s C_p\left(\frac{R_p}{C_s} + \frac{R_s}{C_p}\right)} \tag{15}$$

Because of the parasitic capacitance, the commercial ECIS cannot independently measure the resistance and capacitance of a sample RC circuit, and Z_{ECIS} will change with frequency. The dots shown in Fig. 4 came from measurements of a RC sample connected to the ECIS with a 10-cm and 772-cm cable, respectively. The resistance (R_x) marked on the resistor is 2.21 kΩ (±1%) and the capacitance (C_x) marked on the capacitor is 4.7 nF (±5%). The solid lines in Fig. 4 came from numeric simulation of Eqs. (14) and (15) with R_p = 1017 Ω and C_p = 0.71 nF. The dots from measurements fit Eqs. (14) and (15) very well at frequencies higher than 1 kHz, but the data given by ECIS is not reliable at frequencies higher than 10 kHz because the parasitic impedance of the cable is comparable with the sample impedance. For f < 1 kHz, the impedance of a sample capacitor with 4.7 nF is bigger than 33 kΩ. Since the commercial ECIS system can only handle samples with $|Z_s| < 0.01\ R_o = 10$ kΩ, impedance data given by ECIS are reliable only for frequencies between 1

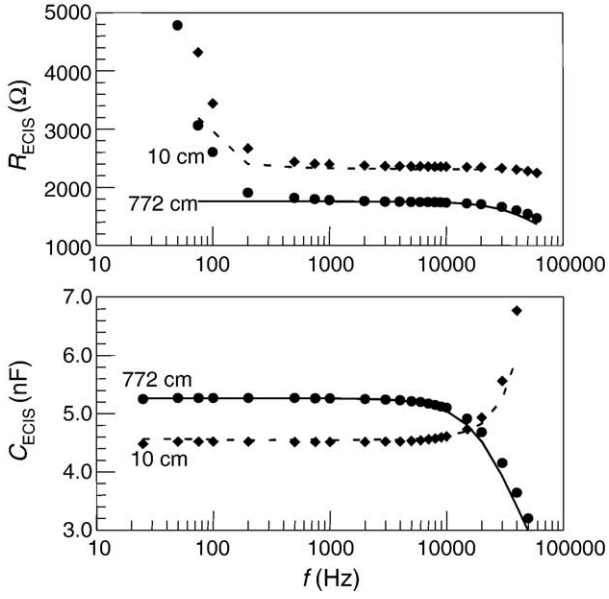

Fig. 4. Effects of cable parasitic impedance to ECIS measurements. The sample was a RC circuit (R = 2.21 kΩ, C = 4.7 nF) and it was connected to the ECIS system by a 10-cm and 772-cm cable, respectively. Dot symbols represented data given by ECIS; solid lines came from numeric simulations (for detail see text); and dash lines came from the modified ECIS.

kHz to 10 kHz. The dash lines in Fig. 4 were derived from the modified ECIS.

For a fixed capacitor (4.7 nF ≤ C_x ≤ 10 nF) in a RC circuit, we changed the resistor (0 ≤ R_x ≤ 10 kΩ) in the sample connected with ECIS by the 125-cm cable, the relationship between the resistance (R_{ECIS}, Ω) at 4 kHz and resistance (R_x, Ω) marked on the resistor is: R_{ECIS} = 0.906 R_x + 77.9. If the cable was cut short to 10 cm, the relationship became R_{ECIS} = 1.004 R_x + 60.1. Although the 10-cm cable insures better results, the 125-cm cable must be used to connect sensing chips in a CO_2 incubator with the control box in the ECIS system. Because the parasitic impedance of the cable and the impedance of sample are not in the same scale, we connected a balance RC circuit (R_b = 2.21 kΩ, C_b = 4.7 nF) in parallel with the sample as shown by the circuit in Fig. 5. A photo of an ECIS modifier with eight balance RC circuits was shown in the figure. The modifier was plugged between the 125-cm cable and the ECIS control box. Before a well on an ECIS chip was filled with culture medium, the impedance of the empty well could be set to infinite. For a sample with infinite impedance, the impedance given by the modified ECIS is $Z_\infty = R_\infty + 1/(j\omega C_\infty)$.

$$\frac{1}{Z_\infty} = \frac{1}{Z_p} + \frac{1}{Z_b} \tag{16}$$

After the culture medium was injected into the well, the impedance of the well was not infinite. For a sample with impedance Z_s connected to the modified ECIS, the impedance directly given by ECIS is $Z_m = R_m + 1/(j\omega C_m)$.

$$\frac{1}{Z_m} = \frac{1}{Z_p} + \frac{1}{Z_b} + \frac{1}{Z_s} \tag{17}$$

From Eqs. (16) and (17), sample impedance Z_s can be derived from Z_∞ and Z_m without knowing Z_p a priori. The sample resistance is equal to Re(Z_s), the real part of Z_s. The sample capacitance is equal to $-1/(\omega \mathrm{Im}(Z_s))$, where Im($Z_s$) is the imaginary part of Z_s.

$$Z_s = \left(\frac{1}{R_m + \frac{1}{j\omega C_m}} - \frac{1}{R_\infty + \frac{1}{j\omega C_\infty}} \right)^{-1} \tag{18}$$

With the 125-cm cable, the modified ECIS can give perfect results about sample impedance from Eq. (18). The calibration result for the modified ECIS at 4 kHz is R_s = 0.999 R_x, with a resulting coefficient of determination better than 0.9999. The dash lines in Fig. 5 were obtained from the modified ECIS. Between 1 kHz to 10 kHz, the modified ECIS system can independently measure resistance and capacitance of RC circuits.

Fig. 6 showed the impedance of two wells measured by the modified ECIS. One well was filled with 0.2 mL DMEM plus 5% FBS, the other well was filled with the same culture medium and its detecting electrode of the well was completely covered by V79 cells. The impedance of a RC circuit (R = 4.7 kΩ, C = 4.7 nF) was also shown in the figure as a reference. For the RC reference circuit, its resistance and capacitance given by the modified ECIS were almost independent of AC frequency. The resistance and capacitance of the well with culture medium slightly decrease with frequency because at higher frequencies, ions in the electrolyte cannot move fast enough. With V79 cells completely covering the detecting electrode, the resistance of the well increased about 300%, but the capacitance of the well decreased less than 28%. At 4 kHz, the change of the capacitance was only about 5%. Since the change of the resistance of a well with cells is more significant than the change of its capacitance, we will focus only on resistance of wells on ECIS chips.

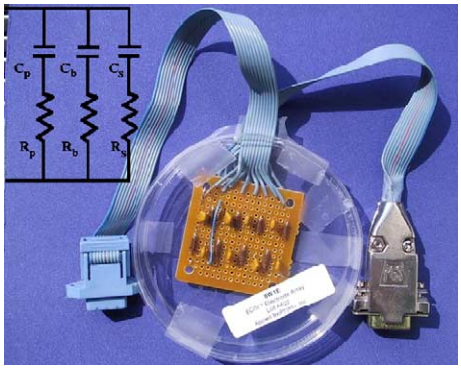

Fig. 5. Photo of one of two ECIS Modifiers and its connection with impedance of sample. Each modifier has eight balance R_bC_b circuits with R_b = 2.21 kΩ, C_b = 4.7 nF. R_pC_p came from the 125-cm cable connecting an ECIS chip (R_p ~ 1 kΩ, C_p ~ 0.2 nF). R_s and C_s were equivalent resistance and capacitance of an ECIS well.

Monitoring cell growth in real-time

Cell culture

A Petri dish inoculated with ~5 × 10^5 V79 cells was incubated in an incubator at 37 °C containing 5% CO_2 for pH and humidity control. The Dulbecco's modified Eagle's medium (DMEM; Gibco BRL, Grand Island, NY) for the cell culture was supplemented with 5% fetal bovine serum (FBS, Sigma). After 48 h, cell suspensions were prepared using 0.05% (v/v) trypsin and cell viability was assessed using the trypan blue exclusion technique (Freshney, 1987).

Electrode coating and cell inoculation

First two new 8W1E chips with 16 empty wells were connected to the modified ECIS system to measure Z_∞. Then, 0.1 mL fibronectin (0.1 mg/mL, prepared in 0.85% NaCl) was admixed into each well to coat the detecting gold electrodes. The chips were placed in CO_2 incubator at 37 °C for 60 min to ensure complete protein adsorption. After

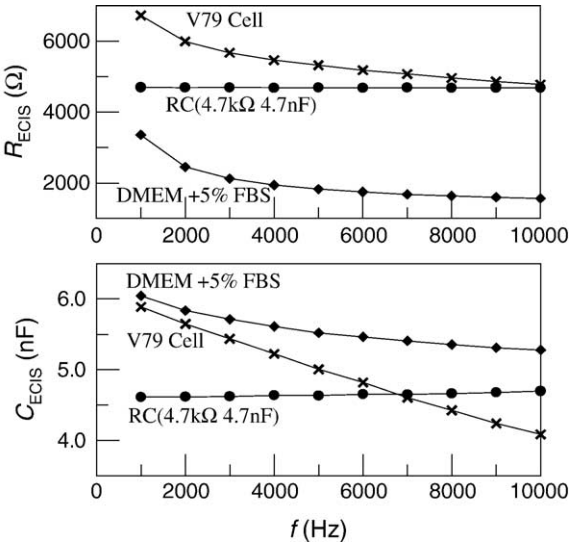

Fig. 6. Resistance and capacitance of two wells filled with 0.2 mL DMEM plus 5% FBS. The detecting electrode of one well was completely covered by V79 cells; the other was blank. The resistance and capacitance of a RC circuit were shown as references.

washing the wells with deonized water, 0.2 mL culture medium (DMEM + 5% FBS) was injected into each empty well and the impedance baseline of each well was monitored for 4 h. At last the wells were emptied, washed with deionized water, and 0.2 mL cell suspension was inoculated into each well.

The amount of protein adsorbed on gold electrodes of ECIS was inferred from a surface plasmon resonance (SPR) biosensor BIAcore 1000 (Biacore AB, Uppsala, Sweden) with a bare gold film evaporated on a glass chip. Fig. 7 showed the adsorption processes of fibronectin. In 0.85% NaCl, the baseline was 6500 RU. Fibronectin solution flowing in the chamber of BIAcore increased θ_{SPR}. After the chamber was washed with saline, water and saline, the resonance angle shifts ($\Delta\theta_{SPR}$) for fibronectin was 3500 RU (0.35°). From protein adsorption processes, it could been seen that 30 min was sufficient for saturated adsorption of the protein on gold surface, and water could not wash the protein away from the gold surface. The surface concentration of fibronectin on the gold surface was 3.5 ng/mm^2. From the fibronectin molecule weight (440,000 g/mol), a fibronectin molecule on the gold surface occupies 209 nm^2. As illustrated by scanning electron microscopy (Engel et al., 1981), fibronectin possesses a V-shape with a length of 130 nm and a thickness of 2–3 nm. The physical area of fibronectin is at least 260 nm^2, which is bigger than the area that was occupied by fibronectin on gold surface. Fibronectin molecules adsorbed on gold surfaces might form a net in which there were overlaps among the fiber molecules.

Cell counting

One hour after inoculation, the chips were taken out from the incubator and placed on an inverted microscope (Wilovert S AFL, Hund, Germany) enhanced with color digital camera (KP-D50U, Hitachi, Japan). Digital photos of detecting electrodes were taken, and these photos were used for counting the initial number (N_o) of cells attached on each detecting electrode. The chips were then brought back to the incubator to continue the experiment and the final cell counting was performed at 25 h or 41 h. For more prolonged incubation, it was somewhat difficult to have precise cell counting as cells became very thin and flat and were occasionally observed to adhere to their neighboring cohorts. In order to facilitate cell counting and microscopic examination, EDTA (0.4 mL, 10 mM in PBS buffer) was added to each well at the end of cell culturing. In EDTA, cells change shapes from flat to round in a course of 15 min so it is easy to distinguish each cell attached on an electrode.

A mathematic model for V79 cell proliferation

Because ECIS only detects cells that attach and spread on the detecting electrode, it is of importance to determine the cell number $N(t)$ during the course of experiments. Cells inoculated in a well require about 30 min to descend to the bottom of the well. After touching the detecting gold electrode precoated with fibronectin, cell–protein adhesion takes place and this process is mediated by integrins on the cell membrane. The experimental data showed that $N(t)$ at t = 25 h and 41 h were proportional to the initial number N (1 h) of attached cells as shown in Fig. 8. At the beginning of cell culture, the number of cells inoculated on a detecting electrode is N(1 h), at t = 25 h and 41 h, the number of cells increase to N(25 h) = 2.87N(1 h) and N(41 h) = 6.12 N(1 h).

Considering the time (τ) required for cells to recover from the disturbance caused by inoculation to a normal growing stage, the cell number on the detecting electrode during the course of experiment should be described as $N(t) = N_o(1 + \eta)^{t - \tau}$. As τ is significantly greater than 1 h, the cell number counted at 1 h into the experiment could

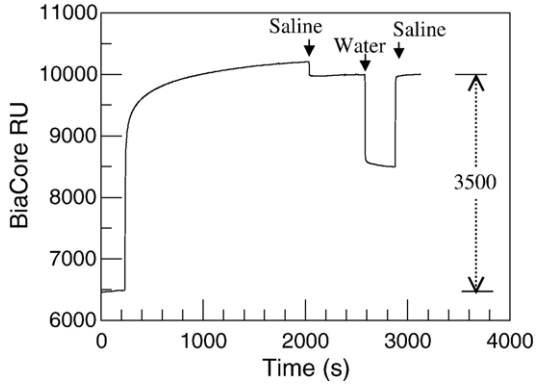

Fig. 7. The amount of fibronectin absorbed on gold surface measured by surface plasmon resonance biosensor (BIAcore 1000) was 3.5 ng/mm^2.

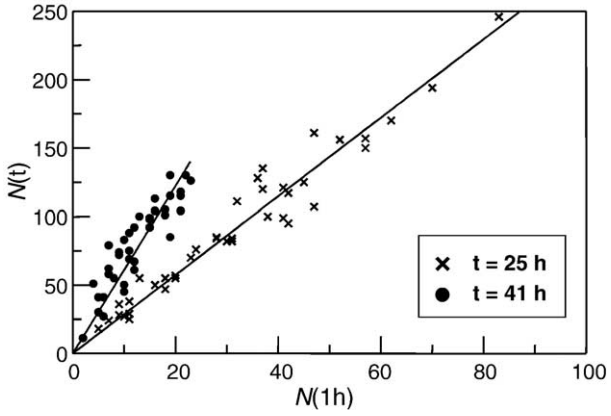

Fig. 8. Proliferation of V79 cells on detecting electrodes in wells of 8W1E chips.

be considered as N_o. Based on the experimental data obtained at 25 h and 41 h, η and τ were estimated to be 4.85% and 2.7 h, respectively. Therefore, the number of V79 cells growing normally on detecting electrodes coated with fibronectin can be expressed as

$$N(t) = N_o(1 + 4.85\%)^{t - 2.7} \quad (19)$$

An independent experiment was also conducted to examine the growth of V79 cells growing in Petri dishes (ϕ 50 mm). After 48 h into the cell culture, the average ratio between N (t = 48 h) and N_o was experimentally determined to be 8.14 (n = 29, s = 1.51), which agreed with the value estimated by Eq. (1) (8.363) for the cell growth in the tissue well. The t test further confirmed that there was no significant difference between the two ratios at α = 0.05. Therefore, the cell growth in Petri dishes and ECIS tissue wells was confirmed to exhibit the same growth rate with a doubling time of 14.6 h. From the information provided by ATCC (Manassas, VA 20108 USA), the generation time of V79 is 12 to 14 h.

Responses of ECIS to cell number

Although the ECIS system can simultaneously measure sample resistance and capacitance, only the resistance changed significantly during cell culture. Fig. 9 described the relationships between resistance change $\Delta R_s(t)$ and the number of cells attached on a detecting electrode at t = 41, 25 and 5 h. For $N(t) < 100$, $\Delta R_s(t)$ was proportional to the cell number attached on the detecting electrode, $N(t)$. At t = 5 h, 25 h, and 41 h, the average value of $\Delta R_s(t)/N(t)$ was estimated to be 42.7 Ω (s = 10.1, n = 71), 44.2 Ω (s = 7.5, n = 24), and 43.2 Ω (s = 11.7, n = 18) per cell, respectively. According to the t test, there was no significant difference among these averages at α = 0.05. At the beginning of cell culture ($t \le 5$ h), cells attached on the detecting electrodes separate from each other because they can be counted easily under the microscope. After 25 h incubation, some or all the cells on the detecting electrodes form a confluent film in which cells attach to each other. Since the contribution of each cell to $\Delta R_s(t)$ was independent of time, the resistance change during cell culture is contributed by the attachment of cells on detecting electrodes coated with protein, not by attachment between cells in the confluent film.

When $N(t) > 100$, $\Delta R_s(t)$ no longer changed with an increase in the cell number. The minimum number of normal V79 cells to completely cover an 8W1E detecting electrode coated with fibronectin was reported to be 93 from our previous work (Xiao et al., 2002). This result was not completely unexpected with respect to the size of V79 cells (~30 μm) vs. the surface area of the detecting electrode. The detecting limit of ECIS to the number of cells attached on a detecting electrode can be explained by a full confluency. Experimental data obtained also illustrated that when $N(t) \le 80$ and t = 5, 25, 41 h, the linear relationship was established as $\Delta R_s(t) = 41.5N(t)$ with a correlation coefficient $r^2 > 0.96$. Consequently, the response function of ECIS using V79 cells ($N(t) \le 80$) growing on fibronectin coated 8W1E sensing chips can be described as

$$f(t) = \frac{\Delta R_s(t)}{N_o} = 41.5(1 + 4.85\%)^{t - 2.7} \quad (20)$$

The response function $f(t)$ can be defined as ECIS sensitivity. At the beginning of cell inoculation in a well on an ECIS chip (t = 0), there is no cell on the detecting electrode, so the resistance change is equal to zero. In about 0.5 h, all cells in 0.2 mL cell suspension descended onto the bottom of the well. While cells were attaching and spreading onto the detecting electrode of the well, the resistance continuously increased with time.

About 1 h into the experiment, the resistance change contributed by each cell attached on the electrode was around 41.5 Ω. During $1 < t < \tau$, the resistance of the well did not change significantly. Because of mitosis after $t > \tau$,

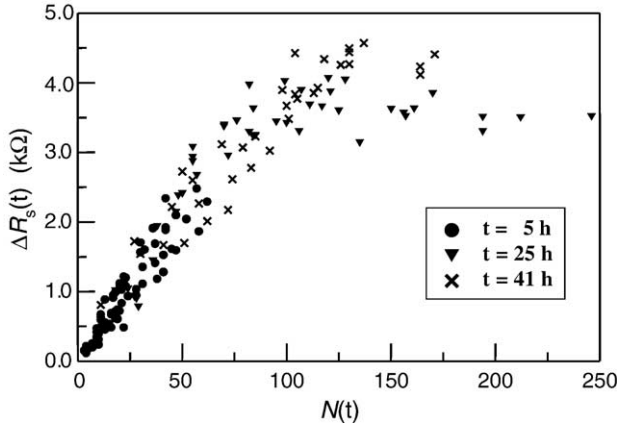

Fig. 9. Relationships between resistance change and the number of cells attached on a detecting electrode at t = 5 h, 25 h and 41 h. For $N(t) \le 80$, the average resistance change contributed by each cell is 41.5 Ω.

the increase in the number of cells obeys Eq. (19) and up to a certain cell number, the ECIS response should be proportional to the cell number. Fig. 10 shows the response functions of the V79 cells with the initial cell number N_o = 12, 9, 11, 31, 47, and 83. In general, with the cell number $N(t) \leq 80$ and $t \geq \tau$, the ECIS response function could be well described by Eq. (20) as illustrated by the smooth curve in the figure. The validity of Eq. (19) was confirmed with N_o = 31 and 47 for the estimation of $N(t)$ = 89 at 25 h and $N(t)$ = 84 at 15 h. In these two cases, the ECIS measured data were well described by Eq. (20) provided the incubation time was less than 25 h and 15 h, respectively. Later, the values of these response functions did not change with time significantly due to the formation of the confluent layer. However, when the initial cell number was very high, 83, (last curve from the top), the response function measured $f(t)$ completely deviated from Eq. (20) right after cell inoculation. For inoculation with high cell populations, the electrode could be completely covered by these cells immediately, and the resistance change of the well approached the upper limit (~4 kΩ) almost instantly. This was the rationale behind the observation that inoculation with higher initial cell numbers resulted in lower responses in the $\Delta R_s/N_o - t$ graph.

The measured response function obtained by ECIS displayed a significant fluctuation to reflect cell motion and viability. The noises or fluctuations of the $\Delta R_s(t) - t$ curves reflected cellular events, not electrical noises of the ECIS machine, because dead cells resulted in very smooth $R_s(t) - t$ curves. It can be seen that the less the number of cells attached on a detecting electrode, the bigger the fluctuation on the $\Delta R_s(t) - t$ curves. The fluctuation on the $\Delta R_s(t) - t$ curves was related to the number of cells attached on a detecting electrode (Fig. 10). These fluctuations might come from cell endocytosis, phagocytosis, and other cellular activities. During these events, there are materials that diffuse in or out of cells; the conductivity of the cell membrane might change rather randomly. When more cells adhered to the detecting electrode, the random conductivity change of each cell could be averaged, resulting in lower fluctuation. Indeed, a series of experiments was conducted using custom ECIS chips with detecting electrodes of 25 μm diameter. Only very few cells were observed to adhere to such small electrodes and the fluctuation in the signal response could reach 50% of its signal background.

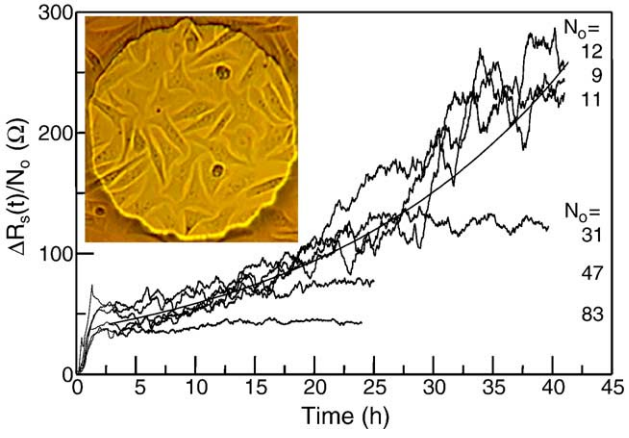

Fig. 10. The response functions of ECIS to V79 cells during normal cell culture procedures. The smooth curve was derived from $f(C,t) = 41.5(1 + 0.0485)^{(t\ -\ 2.7)}$. The number of initial attached cells (N_o) on the detecting electrode at t = 1 h is: 12, 9, 11, 31, 47, 83 (top to bottom). The inset was a photo of V79 cells growing on a detecting electrode coated with fibronectin.

Adding a toxicant to cell suspension

Cadmium chloride, mercury chloride, BAK and sodium arsenate were dissolved in 0.85% NaCl (0.15 M) to a concentration of 10 mM and used as the stock solutions. In a doubling dilution series, 0.5 mL of the stock solution was used to obtain a variety of diluted toxicant solutions. The diluted solutions (C_n) with volume V (10 μl ≤ V ≤ 20 μl) were added to a microtube consisting of 1000 μl cell suspension (~2.5 × 10^5 cells/mL). After thorough but gentle mixing, 0.2 mL of the resulting solution was introduced to each tissue culture well. The final toxicant concentration in the culture well is estimated as $C_nV/(V + 1000)$. TNB was dissolved in dimethyl sulfoxide (DMSO, Sigma) and preliminary studies showed that below 0.35% v/v, DMSO exhibited no effect on the V79 NR cytotoxicity assay. Therefore, 10 μL TNB (0–160 μM prepared in DMSO) was added to 5 mL cell suspension, so that the resulting DMSO concentration in culture medium was less than 0.2% v/v. The toxicant was admixed with the cell suspension just before cell inoculation.

Neutral red cytotoxicity assay

Neutral red (NR, 3-amino-7-dimethyl-2-methylphenazine hydrochloride) is a weak cationic dye that readily penetrates cell membranes by non-ionic diffusion. It accumulates intracellularly into lysosomes, where it binds with anionic sites in the lysosomal matrix. Living cells can hold NR, but damaged or dead cells cannot retain NR, because their plasma membranes do not act as a barrier to NR any more. Therefore, it is possible to distinguish between viable, damaged, and dead cells. The NR assay was carried out according to the method of Borenfreund and Puerner (1984) with slight modifications. Cells inoculated in individual wells of a 96-well microtitre tissue culture plate achieve approximately 80% confluence at the time of the addition of a toxicant. After reaching the required confluence, the medium is replaced with graded dilutions of a toxicant, filling 4–8 wells per concentration. The plate is incubated for 24 h. After incubation, the medium is replaced with NR-containing medium and the plate is incubated for an additional 3 h to allow for the uptake of the dye. The cells are then rapidly washed with a

solution of 1% $CaCl_2$ and 0.5% formaldehyde. The damaged or dead cells would lose their ability to retain NR, which is removed during the wash and fixative step. The dye is then extracted from the intact and viable cells with a solution of 1% acetic acid and 50% ethanol. The plate is left to stand at room temperature for 10–15 min and agitated for about 30 s before measuring the absorbance of the solubilized dye using a spectrophotometer at 540 nm. The NR stock solution (20 mg/mL) was prepared in dimethyl sulfoxide (DMSO, Sigma). The NR working solution (50 μg/mL) was prepared by dilution of the stock solution in 10 mM HEPES-buffered DMEM (pH 7.2). Benzalkonium chloride, a germicidal quaternary ammonium compound, was used as reference toxicant in the NR assay.

Cytotoxicity screening by ABS_{559}

DMEM consists of phenol red, a dye that serves as an indicator of the pH change during cell culturing. Due to the pH change, cells grown on DMEM effect the color of DMEM from red (pH 8.2) to yellow (pH 6.8). If the cell growth is inhibited by a toxicant, the DMEM color remains unchanged or changes very little compared to the negative control. In brief, 1 mL of cell suspension (2.5×10^5 cell/mL) admixed with a toxicant was injected into each well of a 24-well cell culture cluster (Corning, Corning, NY). The cluster was placed in the incubator for 56 h then ABS_{559} (absorbency at 559 nm) of the medium in each well was measured by a spectrophotometer (model DU 640, Beckman, Fullerton, CA). Because this method was simple, it was used to roughly find half inhibition concentration of a toxicant before ECIS assay and neutral red assay.

Safety

Cadmium chloride, sodium arsenate, benzalkonium chloride (BAK), mercury chloride, and TNB must be handled with extreme care. $CdCl_2$ and TNB are carcinogens. Sodium arsenate is a clear, colorless crystalline material and animal tests show that this substance possibly causes fetal malformations. BAK is an antimicrobial germicide that acts by disrupting the cell wall of disease causing bacteria and other microorganisms (Budavari, 1989). $HgCl_2$ is very toxic to the nervous system. To avoid inhalation or any skin contact with these chemicals, protective gloves and clothing were worn. Eye protection using safety glasses is included in the recommended respiratory protection. Preparation and handling of these materials were performed in an exhaust hood equipped with ventilation. It is necessary to contain and dispose of these chemicals as hazardous waste.

ECIS response functions of V79 to toxicants

The adhesion of mammalian cells to ECM protein is mediated by integrins, a family of membrane proteins, which also play an important role in cell–cell adhesion. The recognition and specific binding on integrin to ECM are involved in many complex biological processes. If cells are exposed to a toxicant from the very beginning of an ECIS experiments, the effects of the toxicant to the cell line can be detected earlier. This is one of the advantages of ECIS over other techniques for cytotoxicity assays. When a toxicant at the lethal concentration is mixed with the cell suspension and used for inoculating the tissue culture well, the inhibitory effect on attachment, spreading, mitosis, and cytolysis becomes very complex and time dependent. For an acute toxicant, the majority of cells die instantly and there is no increase in the measured resistance. If cytotoxicity is not very acute, effector cells might still be able to attach and spread on the detecting electrode, leading to an increase in the response function. However, over the lengthy course of toxicant exposure, the attached and infected cells will eventually die and/or cannot bind firmly to the gold electrode, corresponding to a gradual decrease in $f(C,t)$. In an extreme case, the value of the response function $f(C,t)$ approaches zero, an indication of total cell death. In general, the cell growth rate (η) will change with time and the toxicant concentration, that is, $\eta = \eta(C,t)$. Similarly, the contribution of the resistance change by each cell is also a function of time and the toxicant concentration, $k = k(C,t)$. In the presence of a toxicant, the response function measured by ECIS to the cell line should be expressed as

$$f(C,t) = k(C,t)[1 + \eta(C,t)]^{(t-\tau)} \tag{21}$$

When cells are instantly killed by the toxicant, $k(C, t)$ will quickly approach zero, and the real time assay can be performed in a very short time. For less acute toxicants, there is no significant change in $k(C,t)$, however, $\eta(C,t)$ still eventually approaches zero due to the inhibitory effect of the toxicant on the cell growth. The difference of response functions between control and the intoxicated cells might be only observed after many cycles of cell division. In addition, significantly longer time was needed for cytotoxicity assay. For $HgCl_2$, the cytotoxicity effect was concentration-dependent as expected. Above 80 μM, $HgCl_2$ killed V79 cells instantly and the response function f(82.5,t) was measured to be only 10 Ω even after 25 h into the experiment (Fig. 11A). The cytotoxicity effect of $HgCl_2$ on V79 cells was confirmed by microscopic examination of cell counting and morphology. The effector cells subjected to $HgCl_2$ at concentrations above 80 μM could not spread on electrodes. In addition, only a few cells with circular shapes were observed on the detecting electrode (figure not shown). Notice that the fluctuation in the measured resistance ceased when the cells were exposed to high $HgCl_2$ levels (above 75 μM). Such killed cell data supported the biological nature of the fluctuation, a unique feature of viable and attached cells as detected by ECIS. A somewhat similar trend was also observed for

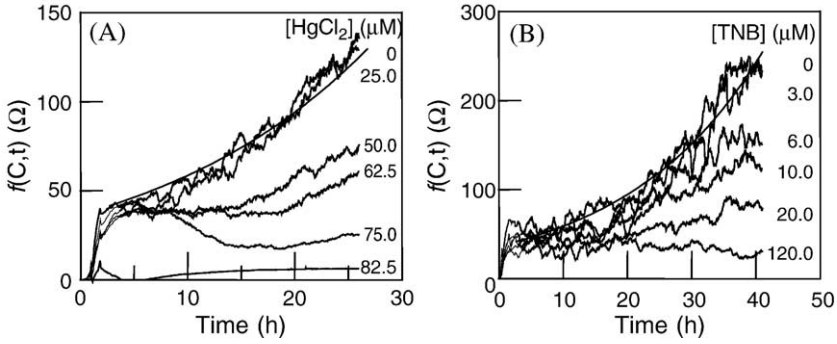

Fig. 11. Some selected response function curves of V79 cells exposed to $HgCl_2$ and TNB whose concentrations were shown in the figure. The two smooth curves were derived from $f(C,t) = 41.5(1 + 0.0485)^{(t\ -\ 2.7)}$.

V79 cells in the presence of TNB as the division of V79 cells was completely inhibited when TNB reached above 80 μM (Fig. 11B). However, the response function of V79 cells displayed a rapid initial drop with an increase in TNB concentration from 6 to 20 μM, followed by a slow decrease in cytotoxicity with an increase in TNB concentration from 20 to 120 μM. Notice also that the assay for TNB was more time-consuming since the cytotoxicity effect of TNB on V79 cells was only obvious after 20–25 h into the experiment.

Half inhibition concentration: $ECIS_{50}$

From the response functions of a cell line to a toxicant, dynamical information of cytotoxicity can be obtained. At a given time on a response function graph shown in Fig. 12, we can draw a vertical line. From a cross point of the vertical line and a response function curve, we can get a point ($f(C,t)$, C). From a series of ($f(C,t)$, C) points came from all the cross points, the relationship between $f(C,t)$ and C can be shown by a graph. Fig. 13 showed relationships between toxicants concentration and values of V79 response functions to $CdCl_2$, BAK and $HgCl_2$ at t = 16 h. The response function $f(0,t)$ measured by ECIS in the absence of the toxicant is defined by Eq. (20), which is a control to a toxicity assay. At t = 16 h, the value of $f(0,t)$ was 78 Ω per cell. Half inhibition concentration of a toxicant to a cell line at time t can be defined as $ECIS_{50}$.

$$\frac{f(\mathrm{ECIS}_{50}, t)}{f(0,t)} = 50\% \tag{22}$$

According to Eq. (22), we draw a horizontal line at $f(C$, 16 h) = 39 Ω. From the cross point of the horizontal line and a $f(C$, 16 h)$-C$ curve, we draw a vertical line which will cross the horizontal axis. The cross point on the horizontal axis determines the half inhibition concentration of the toxicant. Fig. 12 showed that $ECIS_{50}$ of $CdCl_2$, BAK and $HgCl_2$ to V79 at t = 16 h were 4, 13, and 57 μM, respectively.

From $f(C, t)$−t obtained at various concentrations of a toxicant, we got $f(C, T)$−C at any given time $t = T$ during cell culture, then we got half inhibition concentration. The relationship between the half inhibition concentration ($ECIS_{50}$) and time could then be obtained, a unique feature of ECIS. Fig. 13 showed dynamical cytotoxicity information from relationships between half inhibition concentra-

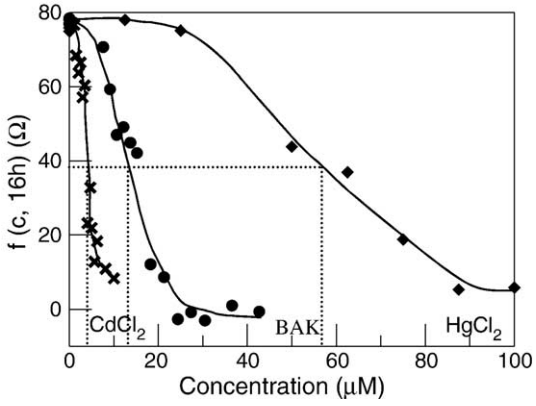

Fig. 12. Relationships between V79 response function and toxicants concentration at t = 16 h. The three toxicants were $CdCl_2$, BAK and $HgCl_2$. From this graph half inhibition $ECIS_{50}$ of a toxicant to V79 could be obtained as shown by the vertical dash lines.

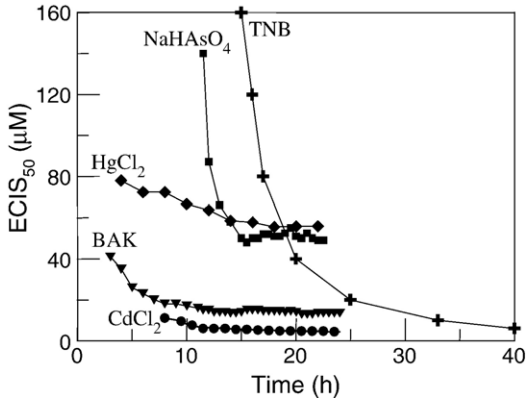

Fig. 13. Dynamical cytotoxicity information from relationships between half inhibition concentration and time for five toxicants: $CdCl_2$, BAK, $HgCl_2$, $NaHAsO_4$, and TNB.

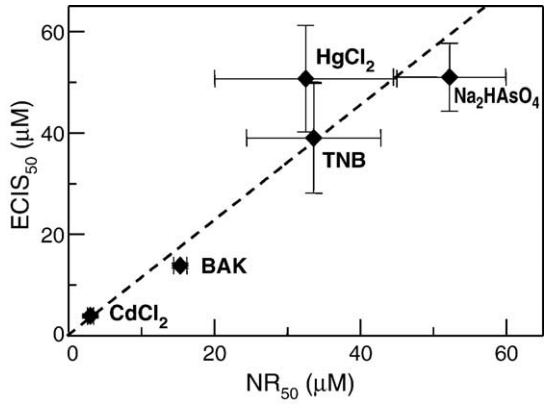

Fig. 14. Comparison of NR_{50} (the half inhibition concentrations measured by neutral red assay) and $ECIS_{50}$ at 24 h after V79 cells incubated with each of five chemicals. Error bars showed the standard deviations of measurements.

tion and time for five toxicants: $CdCl_2$, BAK, $HgCl_2$, $NaHAsO_4$, and TNB. The effect of $HgCl_2$ and BAK could be seen immediately as described earlier with an average half inhibition concentration of 77.5 and 41 μM, respectively. The cytotoxicity of $CdCl_2$, $NaHAsO_4$ and TNB could only be detected after 8, 11, and 16 h after cell inoculation. From 15 h to 20 h after inoculation, $ECIS_{50}$ obtained for TNB to V79 quickly decreased from 160 μM to 40 μM and then leveled off at 6 μM when the experiment was prolonged for another 20 h. At $t = 20$ h, it was difficult to distinguish the effects of $HgCl_2$, $NaHAsO_4$ and TNB to V79 just from $ECIS_{50}$, but from the dynamic toxicity information, it is easy to see their toxic effects.

Neutral red assay is usually used to report chemical cytotoxicity at 24 h after the chemical is incubated with a cell line. NR_{50} is used for the half inhibition of a toxicant measured by neutral red assay In Fig. 14, NR_{50} is compared with $ECIS_{50}$ at 24 h for five chemicals: cadmium chloride ($CdCl_2$), benzalkonium chloride (BAK), sodium arsenate (Na_2HAsO_4), mercury chloride ($HgCl_2$), and TNB. The cytotoxicity data of $CdCl_2$, BAK, and Na_2HAsO_4 were from our previous work. A linear relationship was derived from the figure: $ECIS_{50} = 1.1\ NR_{50}$ with $R^2 > 0.96$. In the ECIS and NR cytotoxicity assays, the standard deviation of $CdCl_2$ or BAK was smaller than 1 μM, and the other three chemicals exhibited a value of ~10 μM. Although both Neutral red assay and ECIS provided similar results, only the latter could provide dynamic cytotoxicity information.

In conclusion, cells growth and division are dynamic and sensitive to environment, especially to toxicants. This study showed that the number of normal V79 cells increased with time and could be described by an exponential function. V79 cells attaching and growing on detecting electrodes coated with fibronectin increased the resistance of the well on an ECIS sensing chip. Before cells completely covered detecting electrodes, the resistance change of an ECIS well was proportional to the cell number attached on the electrodes. As the slope of the linear relationship was constant, the resistance change per the initial number of attached cells measured by an ECIS could be used to monitor the cell growth in real time. An obvious application of the response function is for on-line cytotoxicity assay of known chemicals or unknown ones in the environment. From response functions of cells subjected to different concentrations of a toxicant, the relationship between half inhibition concentration and time could be obtained to provide dynamic information about cytotoxicity.

References

Bell, E., Ivarsson, B., Merrill, C., 1979. Proc. Natl. Acad. Sci. U.S.A. 76, 1274–1278.
Borenfreund, E., Puerner, J.A., 1984. A simple quantitative procedure using monolayer cultures for cytotoxicity assays (HTD/NR-90). J. Tissue Cult. Methods 9, 7–9.
Budavari, S., 1989. The Merck Index, 11th ed. Merck, New Jersey, p. 165.
Dorsey, A., Llaods, F., 1999. ATDSR (Agency for Toxic Substances and Disease Registry) Toxicological Profiles: 1,3-Dinitrobenzene and 1,3,5-Trinitrobenzene. CRC Press, London.
Engel, J., Odermatt, E., Engel, A., Madri, J.A., Furthmayr, H., Rohde, H., Timpl, R.J., 1981. Mol. Biol. 150, 97–120.
Freshney, R., 1987. Culture of Animal Cells: A Manual of Basic Techniques. A.R. Liss, New York.
Giaever, I., Keese, C.R., 1984. Monitoring fibroblast behavior in tissue culture with an applied electric field. Proc. Natl. Acad. Sci. U.S.A. 81 (12), 3761–3764.
Hynes, R.O., 1992. Cell 69, 11–25.
Keese, C.R., Karra, N., Dillon, B., Goldberg, A.M., Giaever, I., 1998. In Vitro Mol. Toxicol. 11 (2), 183–192.
Liedberg, B., Nylander, C., et al., 1983. Surface plasmon resonance for gas detection and biosensing. Sens. Actuators, A, Phys. 4, 299–304.
Pickering, J.G., Chow, L.H., Li, S., Rogers, K.A., Rocnik, E.F., Zhong, R., Chan, B.M., 2000. Am. J. Pathol. 156 (2), 453–465.
U.S. E.P.A., 1997. Support Document for 1,3,5-Trinitrobenzene (TNB), CAS No. 99-35-4. National Center for Environmental Assessment and National Exposure Research Laboratory, Cincinnati, OH 45268. http://www.epa.gov/iris/supdocs/tnb-sup.pdf.
Van der Flier, A., Sonnenberg, A., 2001. Cell Tissue Res. 305, 285–298.
Xiao, C.D., Lachance, B., Sunahara, G., Luong, J.H.T., 2002. An in-depth analysis of electric cell-substrate impedance sensing to study the attachment and spreading of mammalian cells. Anal. Chem. 74, 1333–1339.